Materials Transactions, Vol. 48, No. 10 (2007) pp. 2612 to 2615
Special Issue on Advances in Electron Microscopy for Materials Characterization

Magnetic Macrostructural Study of $L1_0$ Nanocrystalline FePt Alloys by Means of Electron Holography

Weixing Xia[1], Joong Jung Kim[1], Daisuke Shindo[1] and Akihiro Makino[2]

[1]*Institute of Multidisciplinary Research for Advanced Material, Tohoku Univerisity, Sendai 980-8577, Japan*
[2]*Institute for Materials Research, Tohoku Univerisity, Sendai 980-8577, Japan*

$L1_0$ nanocrystalline FePt alloy is directly formed by rapid quenching the melt with simultaneous addition of Zr and B and high coercivity can be obtained in the composition range of $(Fe_{0.55}Pt_{0.45})_{78}Zr_{2-4}B_{18-20}$. Single domain characteristic of the nanocrytalline FePt grains is clarified by Lorentz micorosocpy. Through the measurement of original magnetization curve and hysteresis loop, it is proposed that the mechanism of coercivity belongs to nucleation type. Distributions of lines of magnetic flux at demagnetized state and remanent state for two samples of $(Fe_{0.55}Pt_{0.45})_{78}Zr_4B_{18}$ and $(Fe_{0.55}Pt_{0.45})_{78}Zr_2B_{20}$ are observed by electron holography through ex situ experiment by applying a magnetic field. Obvious differences in the reconstructed phase images indicate the difference of the coercivities of the two samples.
[doi:10.2320/matertrans.MD200705]

(Received April 3, 2007; Accepted May 29, 2007; Published July 19, 2007)

Keywords: *$L1_0$ FePt alloy, electron holography, Lorentz microscopy*

1. Introduction

The ordered $L1_0$ phase of FePt alloy is characterized by a high uniaxial magnetocrystalline anisotropy of 7×10^6 J/m^3 along the easy c-axis.[1)] It has long been anticipated as materials for permanent magnets and magnetic recording. Several reports have been done on mechanism of coercivity of $L1_0$ bulk FePt alloy in order to obtain useful proposal to improve the magnetic hardness. Generally in near equiatomic cast FePt alloy, a high density of extended planar defects such as twins, antiphase boundaries (APB) and stacking faults are formed during the phase transformation from a disordered face-centered-cubic (fcc) to an ordered face-centered tetragonal (fct or L10) by annealing. The mechanism of coercivity was thus proposed to be a pinning type using Kronüller's equation,[2–5)] i.e. the planar defects with thickness less than that of the domain wall work as pinning sites against propagation of domain walls. In ordered Fe-Pt (001) thin film processing with sputtering technique, the structure defects were introduced into the perpendicular recording media to increase the write ability of media.[6)] Generally heating a substrate during deposition or post-annealing for the thin films or the melt-spun alloys is necessary to realize the fcc-$L1_0$ phase transition, however, it has been reported that the ordered $L1_0$ FePt phase can be directly formed by rapidly quenching the melt with the simultaneous addition of B and Zr,[7,8)] high coercivity as 649 kA/m could be obtained in the melt-spun sample $(Fe_{0.55}Pt_{0.45})_{78}Zr_4B_{18}$ at as-quenched state. Although the effects of addition of Zr and B on the microstructure, melting temperature and phase-transition have been described in detail using X-ray diffractometry (XRD),[7)] the investigation of coercivity mechanism is insufficient for the deep understanding of the magnetic hardness of the nanocrystalline FePt alloy. On the other hand, Lorentz microscopy and electron holography are important technologies for analyzing the magnetic microstructure of a variety of magnetic materials.[9,10)] In this paper, the magnetic hardness of directly formed $L1_0$ $(Fe_{0.55}Pt_{0.45})_{78}Zr_{2-4}B_{18-20}$ nanocrystalline alloys are further discussed; the magnetic microstructures of the $(Fe_{0.55}Pt_{0.45})_{78}Zr_4B_{18}$ and $(Fe_{0.55}Pt_{0.45})_{78}Zr_2B_{20}$ are investigated by Lorentz microscopy and electron holography.

2. Experimental Procedure

The original magnetization curve and major and minor hysteresis loop were measured by a superconducting quantum interference device (SQUID) magnetometer with a maximum filed of 7.0 T. Thin foils for the observation of transition electron microscopy (TEM) were prepared by focused ion beam (FIB) method. The Lorentz images and electron hologram were obtained with a JEM-3000F TEM which was equipped a field emission gun and a biprism. The magnetic field in the specimen position could be decreased to 0.6 mT due to a special object lens. The in-plane component of the magnetic flux was visualized by analyzing the phase shift of the electrons traversing the specimen by using the Fourier transform for digital holograms. An ex situ observation was carried out by applying an external field to the specimens using an electro-magnet.

3. Results and Discussions

Figure 1 shows the original magnetization curve and hysteresis loop of $(Fe_{0.55}Pt_{0.45})_{78}Zr_4B_{18}$ at room temperature. The coercivity is 0.831 T (661 kA/m), a little larger than 649 kA/m as exhibited in Ref. 7). The difference is considered to be due to the dispersion of the properties in different part of the melt-spun ribbon, since the $L1_0$ phase was directly formed by the melt-spinning process and the sample was at as-quenched state without going through the annealing treatment. The remanence ratio Mr/Ms is about 0.56, which indicates the isotropic characteristic or randomly oriented FePt grains. Note the original magnetization curve, even a very small magnetic field can induce some magnetization, taking account of the single domain characteristic of the grains shown in the following Lorentz microscopy image, the mechanism of coercivity can be considered as a nucleation type. Figure 2 shows the original magnetization curve and hysteresis loop of $(Fe_{0.55}Pt_{0.45})_{78}Zr_2B_{20}$, the similar shape is

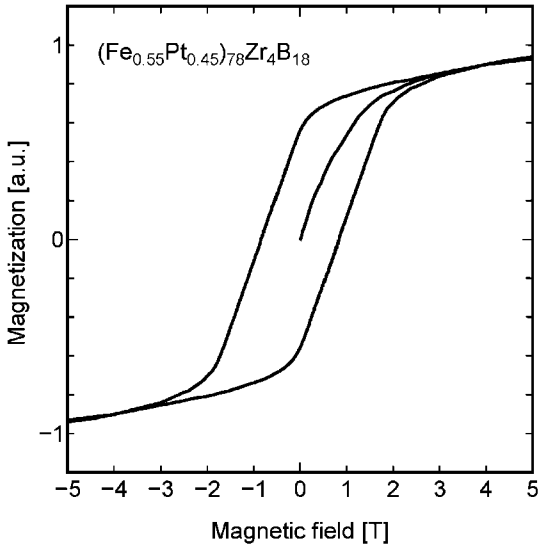

Fig. 1 Initial magnetization curve and hysteresis loop of $(Fe_{0.55}Pt_{0.45})_{78}Zr_4B_{18}$at as-quenched state.

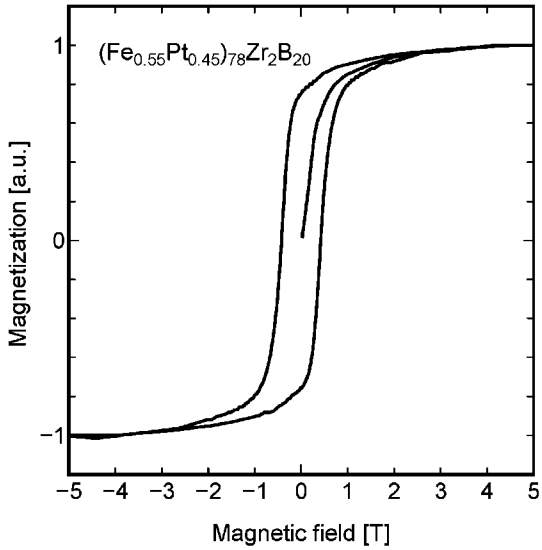

Fig. 2 Initial magnetization curve and hysteresis loop of $(Fe_{0.55}Pt_{0.45})_{78}Zr_2B_{20}$at as-quenched state.

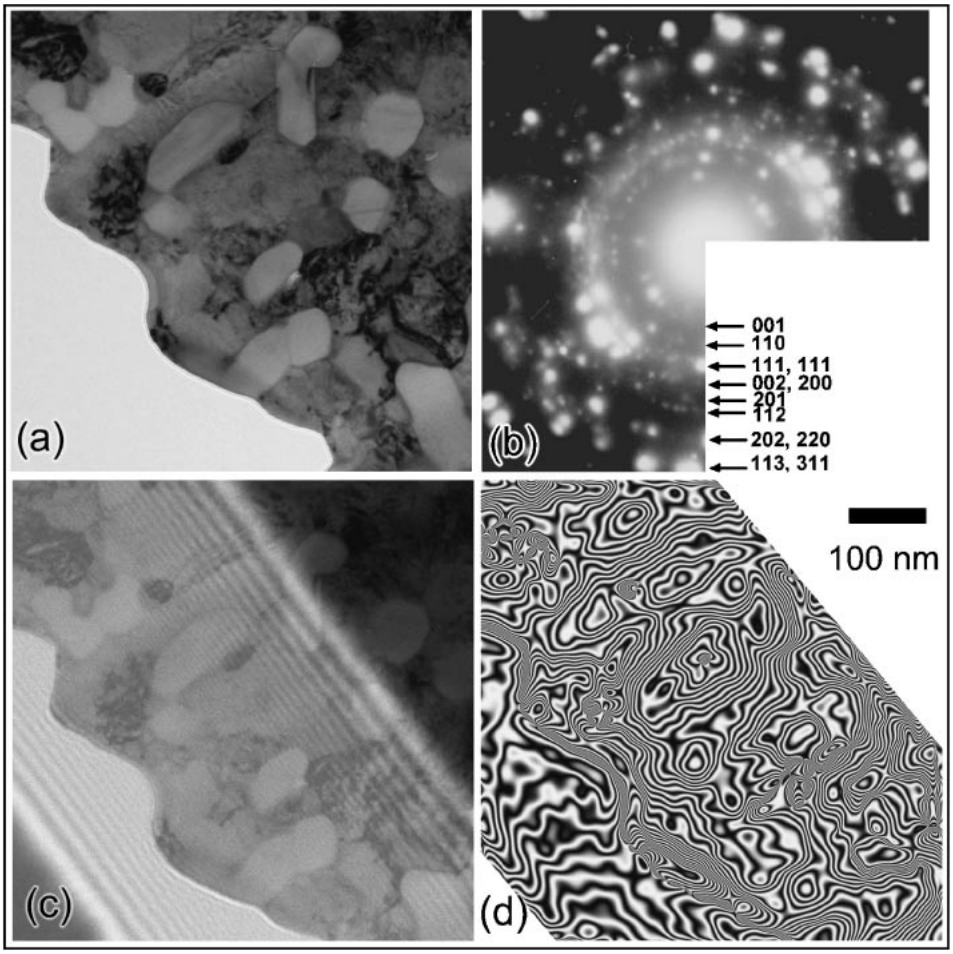

Fig. 3 (a), Fresnel Lorentz image of the sample $(Fe_{0.55}Pt_{0.45})_{78}Zr_4B_{18}$observed at under-focus state. (b), diffraction pattern. (c) and (d) are hologram and the corresponding reconstructed phase image at demagnetized state, respectively.

observed in the original curve as in Fig. 1. The coercivity and Mr/Ms value are 0.427 T (340 kA/m) and about 0.71, respectively. The slope of the loop is larger than Fig. 1, which probably is resulted from the stronger intergranular exchange interaction of $(Fe_{0.55}Pt_{0.45})_{78}Zr_2B_{20}$.

X-ray diffraction profiles indicated that the two samples of the FePt alloys were composed of ordered $L1_0$ phase and a minor segment of the fcc phase.[7] The microstructure was observed by TEM. Figures 3(a) and (b) show the Lorentz images of $(Fe_{0.55}Pt_{0.45})_{78}Zr_4B_{18}$ at under-focus state and

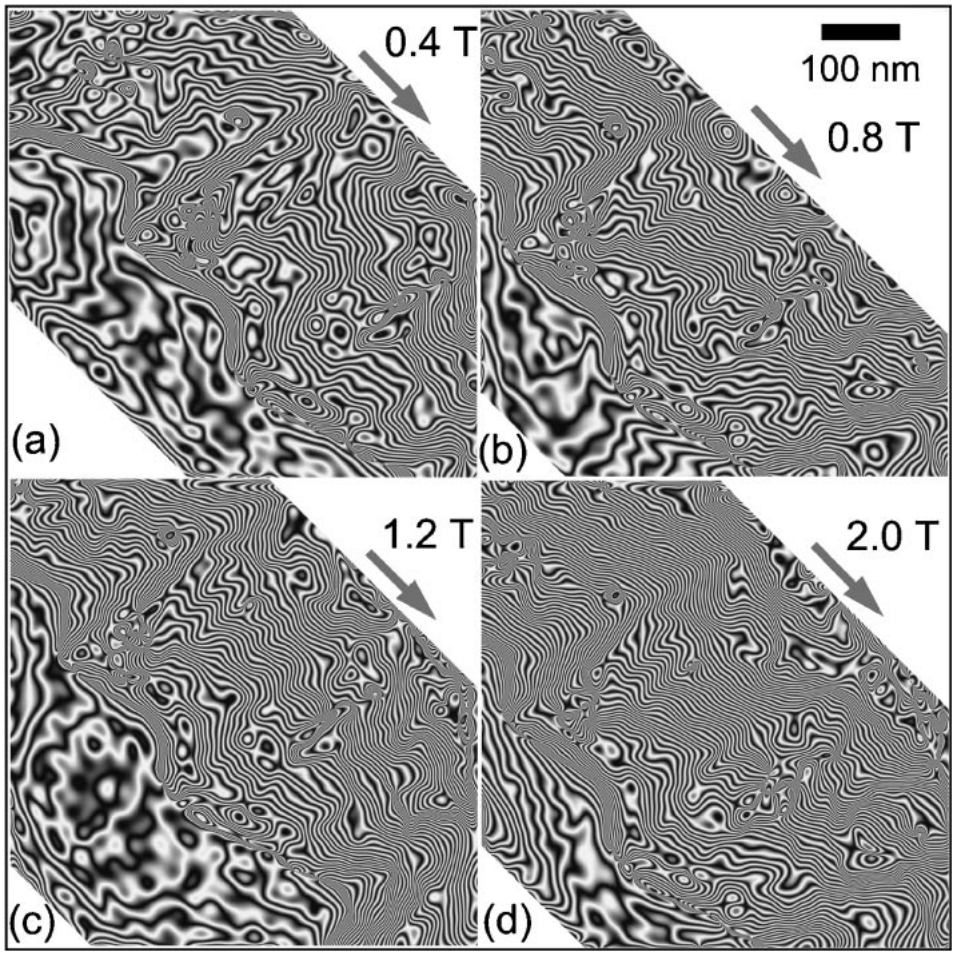

Fig. 4 Reconstructed phase images of remanent states of the sample $(Fe_{0.55}Pt_{0.45})_{78}Zr_4B_{18}$ after magnetic fields (a) 0.4 T, (b) 0.8 T, (c) 1.2 T, (d) 2.0 T are applied.

diffraction pattern within a circle area with diameter of about 2.0 μm, respectively. It is shown that the grain sizes are from 40 nm to 200 nm. Besides the fundamental diffractions of 111, 200, 220 and 311, supperlattice diffractions of 001, 110, 201 and 112 are clearly observed, indicating the composition of $L1_0$ phase and fcc phase. The broadness of fundamental diffractions is resulted from the superposition of the supperlattice diffractions. Although complete Debye-Scherrer rings are not observed due to the small observation area, it can be considered that the grains are randomly oriented. In Lorentz images at under-focus state (Fig. 3(a)) and over-focus state (not shown), no reverse dark-bright contrasts or domain walls are observed inside and outside grains. One thing indicated is that the grains are of single domain characteristic, since the grain sizes are less than the critical single domain grain size of 340 nm.[4] The other thing indicated is that the weaker intergranular exchange interaction than $Nd_2Fe_{14}B$ nanocrystalline materials,[11] which can also be confirmed by the small slope of the hysteresis loop as shown in Fig. 1. Figure 3(c) is the hologram with applied electrical field to biprism of 50 voltages. Figure 3(d) presents the reconstructed phase image obtained by fast Fourier transformation of the hologram, which corresponds to the lines of magnetic flux at the demagnetized state. Except some closure lines, the irregularity distributions of magnetic flux are observed. Since the grains are randomly oriented, it is difficult to distinguish which grain or which part is $L1_0$ phase or fcc phase, however, it can be said that the randomly oriented $L1_0$ phase and the interaction between hard $L1_0$ phase and the soft fcc phase result in the irregularity of the lines of magnetic flux.

The ex situ observation experiments were carried out by applying an external field to the specimen using an electromagnet. The applied field was increased from 0 to 2.0 T (1600 kA/m) in 0.4 T (320 kA/m) steps, the remanent state in each step was observed with electron holography. Figures 4 show the reconstructed phase images at remanent state after magnetic fields of (a) 0.4 T, (b) 0.8 T, (c) 1.2 T and (d) 2.0 T were applied. The directions of the magnetic field are indicated with large arrows in the upper right corner of each figure. When the applied field was less than 0.8 T (640 kA/m), only a little changes of lines of magnetic flux were observed. While it was increased to 0.8 T, a large amount of lines of magnetic flux change their directions to that of the applied field as shown Fig. 4(b). It is interpreted that most $L1_0$ FePt grains with angles of spontaneous magnetization to the applied field larger than 90 degrees reversed their directions. The strength of the applied field has a basic agreement with the coercivity of $(Fe_{0.55}Pt_{0.45})_{78}Zr_4B_{18}$. When the applied field are increased to 1.2 T and 2.0 T, the remanent states have been almost saturated and the lines of magnetic flux have no large change as shown in Fig. 4(c) and (d).

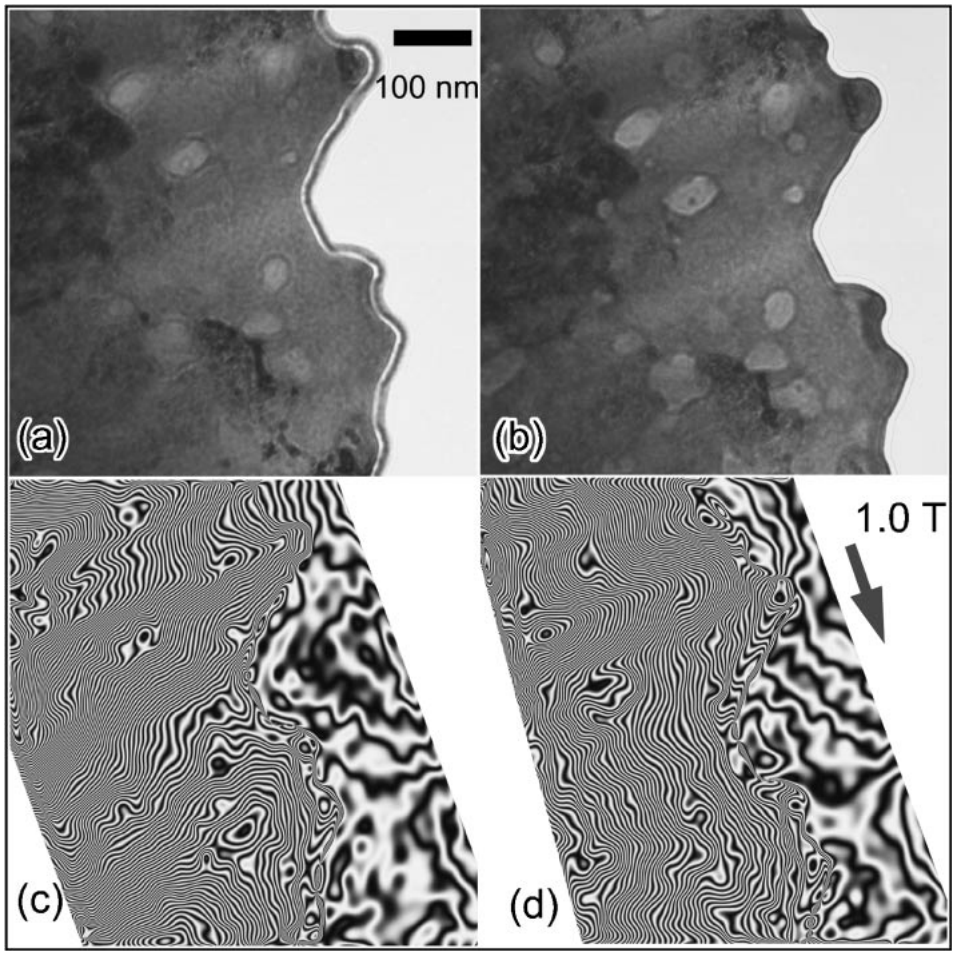

Fig. 5 Fresnel Lorentz images of the sample $(Fe_{0.55}Pt_{0.45})_{78}Zr_2B_{20}$observed at under-focus state (a), and over-facus state (b). (c) and (d) are reconstructed phase images at demagnetized state and remanent state after magnetic field of 1.0 T are applied, respectively.

Figures 5(a) and (b) show the Fresnel Lorentz images of the sample $(Fe_{0.55}Pt_{0.45})_{78}Zr_2B_{20}$ observed at under-focus and over-focus states, respectively. The grain sizes are about 20–100 nm. No domain walls are observed. Fig. 5(c) shows the reconstructed phase image in demagnetized state. Comparing this image to that of $(Fe_{0.55}Pt_{0.45})_{78}Zr_4B_{18}$ shown in Fig. 3(d), quite homogenous distribution of lines of magnetic flux are observed, which infers the smaller coercivity of this sample as shown in Fig. 1 and Fig. 2. The similar ex situ experiments were carried out for this specimen. When the external field was increased to 0.4 T, i.e. near its coercivity, the closure shape of magnetic flux disappeared, finally after 1.0 T was applied it got to the saturated remanent state as shown in Fig. 5(d).

4. Conclusions

The $L1_0$ melt-spun FePt nanocrystalline alloys $(Fe_{0.55}Pt_{0.45})_{78}Zr_4B_{18}$ and $(Fe_{0.55}Pt_{0.45})_{78}Zr_2B_{20}$ were characterized by Lotentz microscopy and electron holography. The results can be summarized into three points as follows.

(1) Single domain characteristic of $L1_0$ Fe-Pt grain was confirmed by Lorentz mircoscopy. Through measurement of original magnetization curve and hysteresis loop, the coercivity mechanism is considered to belong to a nucleation type.

(2) The fluctuation of lines of magnetic flux of $(Fe_{0.55}Pt_{0.45})_{78}Zr_4B_{18}$ in demagnetized state infers the higher coercivity than that of $(Fe_{0.55}Pt_{0.45})_{78}Zr_2B_{20}$.

(3) Through the ex-situ experiment, a basic correspondence between coercivity of the sample and the images of lines of magnetic flux in remanent state was obtained for two samples.

REFERENCES

1) O. A. Ivanov, L. V. Solina, V. A. Demshina and L. M. Magat: Phys. Met. Metallogr. **35** (1973) 81–85.
2) H. Kronmüller and K.-D. Durst: J. Magn. Magn. Mat. **74** (1988) 291–302.
3) J. Bauer, M. Seeger, A. Zern and H. Kronmüller: J. Appl. Phys. **80** (1996) 1667–1673.
4) T. Klemmer, D. Hoydick, H. Okumura, B. Zhang and W. A. Soffa: Scr. Metall. Mater. **33** (1995) 1793–1805.
5) B. Zhang and W. A. Soffa: IEEE Trans. Magn. **26** (1990) 1388–1390.
6) T. Suzuki and K. Ouchi: J. Appl. Phys. **91** (2002) 8079–8081.
7) A. Makino, T. Bitoh and A. Inoue: Mater. Trans. **45** (2004) 2909–2915.
8) T. Bitoh, A. Makino and M. Nakagawa: J. Appl. Phys. **97** (2005) 10H307.
9) D. Shindo: Mater. Trans. **44** (2003) 2025–2034.
10) D. Shindo, Y. G. Park, Y. Gao and H. S. Park: J. Appl. Phys. **95** (2004) 6521–6526.
11) Y. Gao and D. Shindo: J. Appl. Phys. **93** (2003) 8119–8121.